Microreactor Fluidics

DOI: 10.1002/ange.200500792

A Microfabricated Gas–Liquid Segmented Flow Reactor for High-Temperature Synthesis: The Case of CdSe Quantum Dots**

Brian K. H. Yen, Axel Günther, Martin A. Schmidt, Klavs F. Jensen, and Moungi G. Bawendi**

Microfluidic reactors enable a number of advantages over conventional chemical processes including enhanced control of heat and mass transfer, lower reagent consumption during optimization, and sensor integration for in-situ reaction monitoring.[1,2] Reactors are usually fabricated from either silicon, glass, or polymers; those made of silicon or glass are advantageous because they can tolerate a broad range of chemistries and high temperatures. Microreactors for the large class of homogeneous liquid-phase reactions are often based on single-phase laminar flow designs in which reagent streams are brought into contact. However, such designs are limited in terms of slow diffusive reagent mixing and broad residence time distributions (RTDs). Recirculation within segments in a two-phase segmented flow approach (gas–liquid or liquid–liquid) overcomes such limitations by providing a mechanism of exchanging fluid elements located near the channel walls with those at the center.[3–5] This recirculatory motion has the dual effect of narrowing the RTD and improving reactant mixing. In contrast to single-phase designs, segmentation makes it possible to drive reactions to required yields over significantly shorter times owing to the enhanced mixing, while maintaining narrow RTDs.

---

[*] A. Günther, Prof. K. F. Jensen
Massachusetts Institute of Technology
Department of Chemical Engineering
Institute for Soldier Nanotechnologies
77 Massachusetts Avenue, 66–566, Cambridge, MA 02139 (USA)
Fax: (+1) 617-258-8224
E-mail: kfjensen@mit.edu

B. K. H. Yen, Prof. M. G. Bawendi
Massachusetts Institute of Technology
Department of Chemistry
Institute for Soldier Nanotechnologies
77 Massachusetts Avenue, 6–221, Cambridge, MA 02139 (USA)
Fax: (+1) 617-253-7030
E-mail: mgb@mit.edu

Prof. M. A. Schmidt
Massachusetts Institute of Technology
Microsystems Technology Laboratories
Department of Electrical Engineering and Computer Science
Cambridge, MA 02139 (USA)

[**] This research was funded in part by the NSF-CRC program (CHE-0209898), the Microchemical Systems Technology Center, and the U.S. Army through the Institute for Soldier Nanotechnologies (under contract DAAD-19-02-0002 with the U.S. Army Research Office). B.K.H.Y. acknowledges support from the NDSEG Fellowship Program. We thank the staff of the MIT Microsystems Technology Laboratories for assistance with microfabrication.

Gas–liquid rather than liquid–liquid segmented flow offers the most versatility in terms of the range of chemistries that can be performed in a microfluidic system. Gas–liquid flow is preferable for performing reactions at elevated temperatures, as most solvents experience increased miscibility at higher temperatures. Moreover, it is possible to obtain uniform segmentation in gas–liquid flows over a very large range (over two orders of magnitude) of bubble velocities and therefore reaction timescales.[4,5] Liquid–liquid segmented flow systems are operated over a much narrower range with typical droplet velocities varying over one order of magnitude.[3,6] Finally, in gas–liquid segmented flow, the reaction solution is present as a continuous liquid phase within the channel (Figure 1) so that it is possible to inject additional reactants or withdraw reaction aliquots in a continuous, controllable manner. In liquid–liquid segmented flow, the reaction solution is usually the dispersed (droplet) phase; subsequent addition of reactants is challenging, as it requires synchronized merging of discrete droplets.[6] The withdrawal of small aliquots without disturbing the flow is also difficult. Herein, we demonstrate a silicon-based microreactor that incorporates both gas–liquid segmented flow and multiple temperature zones. The reactor represents a general platform for high-temperature synthesis under very well-defined reaction conditions (mixing times and narrow RTDs).

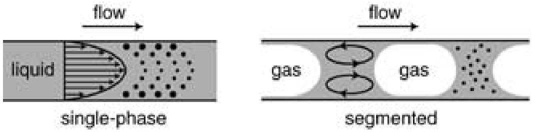

Figure 1. Mixing and residence time distribution (RTD) effects in a) single-phase and b) segmented gas–liquid flow. In the single-phase laminar flow, diffusion is the only means of mixing. As a result of the parabolic fluid-velocity profile, particles near the wall spend more time in the reactor than those in the center, resulting in broad RTDs. In the two-phase case, recirculation within each liquid slug brings material from the wall to the center of the channel. This facilitates mixing, which narrows the RTD, and results in narrower size distributions.

As a model system for the reactor, the preparation of CdSe quantum dots (QDs) was chosen, as the chemistry a) requires high temperatures and b) highlights the advantages of the segmented-flow approach over single-phase and conventional batch processes. In the batch method, semiconductor QDs (diameters = 2–10 nm) are synthesized by the rapid injection of precursors into a heated flask containing a mixture of solvents and ligands.[7–10] Factors such as the injection process, local temperature and concentration gradients, mixing rate, and cooling rate strongly influence QD nucleation and growth, but are difficult to control. Single-phase continuous flow reactors in which precursor solutions are delivered into a heated reaction section have addressed some of these reproducibility problems.[11] However, these reactors suffer from slow mixing and broad RTDs, which are detrimental to the particle size distribution (Figure 1). It has been challenging to adapt QD chemistry to a chip-based segmented flow system owing mainly to the reaction temperatures required (> 250 °C). Liquid–liquid segmented flow has been used to prepare QDs at room temperature in a polydimethylsiloxane device,[6] but solvent miscibility and polymer degradation at high temperatures make it difficult to use this approach to prepare monodisperse, luminescent particles.

The introduction of segmenting gas into heated capillaries has also been implemented, but the uniformity of such gas–liquid flows and their effect on QD formation were not extensively characterized.[12,13] We demonstrate herein the success of our microreactor design in rapid mixing and extremely uniform segmentation behavior at the high temperatures required for QD synthesis. The QD sample size distributions and reaction yields are superior to those attainable in single-phase flow, with the improvement significantly more pronounced at short reaction times. As the improvement is a direct consequence of the rapid mixing and narrow RTD features of segmented flow, the reactor greatly decreases the time required to produce high-quality particles in comparison with existing single-phase approaches. Moreover, the reactor is applicable to a variety of nanoparticle chemistries because it offers access to a wide range of reaction timescales without a compromise in acceptable size distributions.

The reactor shown in Figure 2 allows rapid initial mixing of the precursors, controlled QD growth, and on-chip quenching of the reaction. The silicon reactor accommodates a reaction channel length of approximately 1 m (hydraulic diameter ≈ 380 μm) and two shallow side channels for collecting reaction aliquots. A halo etch region makes it possible to localize multiple temperature zones for reaction (> 260 °C) and quenching (< 70 °C) on the device. Precursor solutions are delivered separately into the heated section and an Ar gas stream introduced further downstream results in a segmented gas–liquid flow. Recirculation within the liquid slugs rapidly mixes the heated precursors, thereby initiating the reaction. The fluids initially pass through a meandering section to induce good mixing across the channel[3–5] before reaching a longer straight-channel section where the majority of the particle growth occurs. The reaction is stopped when the fluids enter the cooled outlet region of the device. The segment lengths are very uniform during conditions of a typical QD synthesis (Figures 2 a and b). Figure 2 c shows a long-time-exposure image of the cooled outlet region of the device under continuous UV excitation. At the high reaction temperatures, the QD photoluminescence (PL) is completely quenched (top portion of Figure 2 c), but once the fluid reaches the cooled region (< 70 °C), yellow PL is observed. The image illustrates our ability to maintain the required ≈ 200 °C temperature gradient within a single reactor chip.

The quality of the segmentation shown in Figures 2 a and b deserves further discussion, as the slug-length distribution can contribute to the RTD and therefore the ultimate QD size distribution. We systematically examined the slug statistics over a range of flow conditions by varying either the total fluid flow rate under conditions of constant gas-to-liquid flow rate (v_g/v_l) or by varying v_g under conditions of constant v_l.[14] The resulting liquid slug-length distributions over this range of residence times are shown in Figure 3 a. The liquid lengths are on the order of the channel hydraulic diameter and typically have a relative standard deviation of ≤ 10 %.

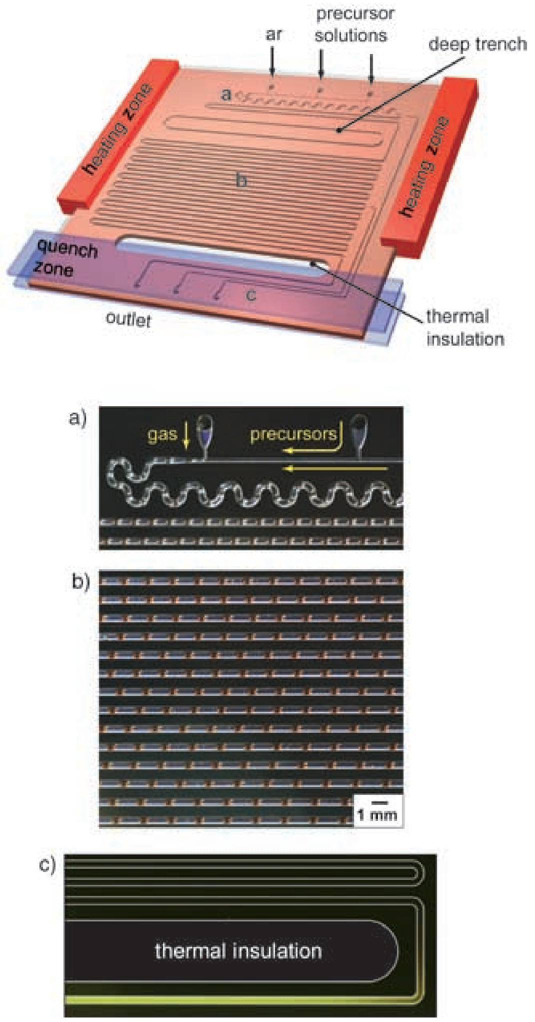

Figure 2. Reactor with heated reaction region and cooled outlet zone: a through-etch section ensures that the two regions are thermally isolated; a) heated inlets and b) main channel section: red segments = QD reaction solution; dark segments = Ar gas; c) time-exposure image of the cooled outlet region under UV irradiation. $T = 260\,°C$, $\nu_g = 60\ \mu L\,min^{-1}$, $\nu_l = 30\ \mu L\,min^{-1}$, Se/Cd = 5.0.

This dispersion in the slug lengths is small enough so that it does not contribute to the overall RTD.[15] The resulting spectra of the QD samples indicate narrow size distributions (Figure 3b) and are similar to the best samples obtained by the batch process. The band-edge absorbance and several higher transitions are clearly resolved, and the PL line widths remain narrow over the entire range of flow rates. In the figure, the PL full-width-at-half-maximum (fwhm) varies between 28 and 31 nm (112 and 119 meV, depending on wavelength).

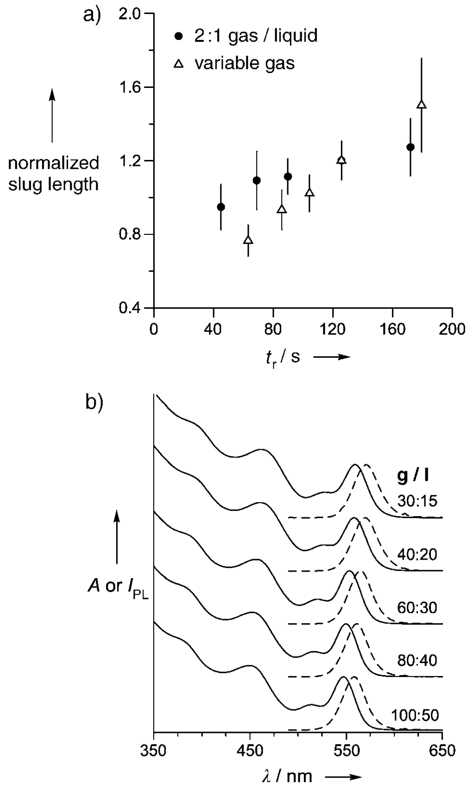

Figure 3. a) Ratio of average liquid slug length to hydraulic diameter (≈380 µm) over a range of flow rates (residence times, t_r) at 260 °C; error bars indicate the standard deviation of the liquid length for a given flow condition; ● = gas/liquid flow rates of: 100/50, 80/40, 60/30, 40/20, and 30/15 µL min^{-1} (ratio kept equal to 2); △ = flow rates of: 100/20, 80/20, 60/20, 40/20, and 30/20 µL min^{-1} (liquid flow rate kept at 20 µL min^{-1}). b) Absorbance (——) and photoluminescence (PL) (-----) spectra for QDs prepared under the flow conditions represented by (●) in part a).

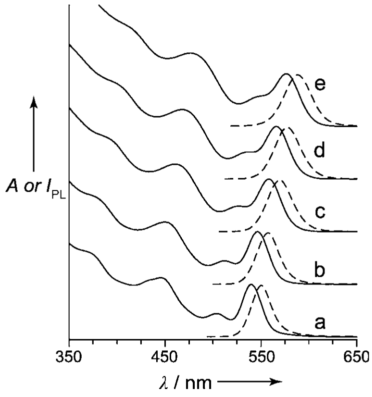

Figure 4. Absorbance (——) and photoluminescence (PL) (-----) spectra for QDs obtained by varying the precursor feed ratio ($T = 260\,°C$). The total gas and liquid flow rates were kept constant ($\nu_{l(Se)} + \nu_{l(Cd)} = 20\ \mu L\,min^{-1}$, $\nu_{g(Ar)} = 40\ \mu L\,min^{-1}$). Spectra correspond to the flow rates ($\nu_{l(Se)}/\nu_{l(Cd)}$) and resulting concentration ratios (Se/Cd) of a) 3.0 and 15, respectively; b) 1.67 and 8.3; c) 1.0 and 5.0; d) 0.60 and 3.0; e) 0.33 and 1.7.

In Figure 3b, the QDs were prepared with a constant precursor composition and represent a fairly limited spectral range (< 10 nm variation in band-edge position). As discussed previously, it was found that size tuning is more readily accomplished through variation in the ratio Se/Cd rather than the reaction time.[12] Figure 4, illustrates such an effect from varying the Cd and Se precursor flow rates while the keeping the total liquid and gas flow rates constant (at 20 and 40 µL min^{-1}, respectively). In contrast to Figure 3b, a change in the ratio Se/Cd from 15 to 1.7 made it possible to tune the effective band gap of the QDs over a much larger spectral range of ≈40 nm yet maintain narrow size distributions. The average QD radius decreases with an increase in the Se/Cd ratio owing to the strong dependence of the nucleation rate on the precursor ratio. The samples represented in Figure 4 were produced by using the same temperature (260 °C) and mean residence time (≈140 s). By varying the temperature and reaction time in addition to the precursor feed ratios, it would be possible to tune the effective band gap over an even larger spectral window.

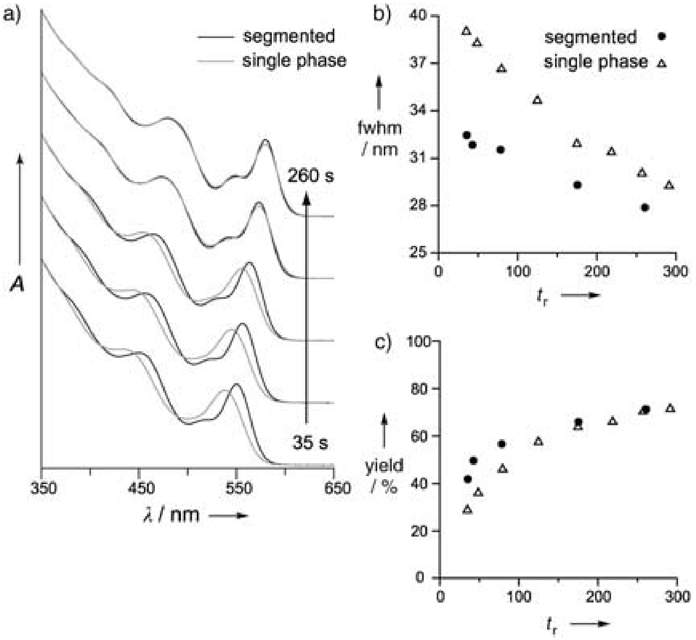

Figure 5. a) Absorbance spectra of QDs prepared with segmented and single-phase flow. Each pair of spectra corresponds to approximately the same mean residence time. b) PL full-width-at-half-maximum (fwhm) and c) reaction yield of QD samples prepared in segmented (●) and single-phase (△) flow. For segmented flow, ν_g/ν_l was varied between 15/10 and 100/40 µL min^{-1}. For single-phase flow, ν_l was varied between 34 and 250 µL min^{-1}. $T = 280$ °C, Se/Cd = 1.0.

In general, it was found that spectra of QDs produced in single-phase operation ($\nu_g = 0$) were significantly broader than those obtained with gas–liquid flow. The poorer performance observed in the single-phase case results primarily from the combination of two effects: initial mixing and broad RTD. In single-phase flow, the two precursor streams combine slowly by diffusion, in contrast to the convective mixing induced by the introduction of a segmenting gas.[16] Slow initial mixing makes it difficult to realize a rapid nucleation burst, and the resulting QD samples are polydisperse. Once the reagents are completely mixed, the RTD effect is still present; QDs near the channel wall spend a longer time in the reactor than those in the channel center. In segmented flow, recirculation within the liquid brings fluid from the channel wall to the center which facilitates rapid mixing, lower dispersion in residence times, and therefore narrower QD size distributions (Figure 1).

To isolate the RTD contribution from the effects of initial mixing, we cooled the inlet region of the reactor and premixed the precursors inline with a miniature convective mixer. A deep trench feature (Figure 2) allowed us to keep the inlets thermally isolated from the main reaction channel. Cooling the inlets ensures that the pre-mixed precursors do not react until they reach the heated reaction section. In this way, we eliminated the effect of initial reagent mixing and were able to directly observe the RTD effect on the QD size distribution. The spectra in Figure 5a illustrate the improvement of the size distribution resulting from segmentation. Figure 5b is a plot of the fwhm of the PL peak for samples prepared at several flow conditions (mean residence times). For reaction times shown in Figure 5b, the PL fwhm varies between 28 and 32 nm (99–128 meV) for segmented flow, and 29 and 39 nm (104–158 meV) for single-phase flow. In both plots in Figure 5b, the PL peak width decreases with time, and this general trend (size distribution focusing) has been explained as evidence of the presence of a mass-transfer component in the particle growth rate.[17,18] However, the absorbance and PL spectra of QDs produced in gas–liquid flow are generally sharper in than those produced in single-phase scenarios. Furthermore, the difference shown in Figures 5a and b between single- and two-phase flow becomes more pronounced at shorter timescales. This behavior at short times results from the fact that the RTD broadens significantly with flow rate in single-phase flow,[12] whereas the RTD does not have such a strong flow-rate dependence in the segmented case. Notably, cooling the inlets is not the normal mode of operation for the device. Upon introduction of the gas at low temperature, the slug uniformity is substantially poorer than the uniform segments shown in Figures 2a and b. This flow destabilization results primarily from rapid expansion of gas and the large change in liquid viscosity when the fluids reach the heated section. In spite of such non-uniform segmentation, a significant improvement in QD size distribution is still observed.

Figure 5c reveals an additional reason for the larger improvement in size distribution at shorter reaction times. In segmented flow, the mixing timescale that is governed by recirculation within liquid slugs decreases almost linearly with flow rate.[5] Therefore, a shorter reaction time (faster flow rate) is compensated by more intense stirring, and vice versa. The inverse relationship between stirring intensity and reaction time is manifested in the reaction yield curves shown in Figure 5c. At shorter times (high flow rates), the QD reaction is driven to higher yields than those of the single-phase operation. The increased growth rate causes the QD population distribution to focus more quickly than in the single-phase case. Consequently, the difference in the two curves in Figure 5b is more pronounced at short times. At lower flow rates, the recirculatory stirring is slower, but the reaction time is longer, thus the yield curve converges with that for single-phase flow. Even at the longest reaction times (when the yields are similar for the two cases), the PL spectra for gas–liquid flow is still somewhat narrower, indicating that the improved RTD effect on size distribution is still present. In summary, the synthesis of acceptable QD samples by the single-phase approach requires long reaction times to allow the size distribution focusing and narrowing of the RTD time to fully develop. In segmented flow, the enhanced mixing accelerates the particle formation process, thereby decreasing the time required for focusing the size distribution, and a narrow RTD is sustained even at high flow rates. For example, from Figure 5 b, the narrow size distribution obtained in 42 s with segmented flow requires over fourfold more time (≈ 175 s) to achieve with single-phase flow.

In conclusion, we have designed a gas–liquid segmented flow reactor with multiple temperature zones. The reactor is applicable to a range of chemistries because it is possible to operate at high temperatures, yet maintain excellent mixing and RTD characteristics. To illustrate the unique features of the design, it was applied to the synthesis of CdSe QDs. Under the reaction conditions reported, segmentation is very uniform and the resulting monodisperse samples exhibit excellent optical properties. Relative to single-phase flow, the enhanced mixing and narrow RTD characteristics of the reactor result in a significant improvement in reaction yield and size distribution, especially at short reaction times. Such attributes are highly desirable from the standpoint of chemical production, as it is possible to increase throughput without sacrificing narrow size distributions. Furthermore, the reactor is applicable to particle systems in which the optimal reaction timescales are shorter than that of CdSe QDs, in contrast to single-phase devices, which are limited to long reaction times. In addition to its use as a synthesis tool, variation of the mean slug velocity and length in the reactor channel provides a way to reproducibly control the mass-transfer rate during particle formation, which is not possible in single-phase flow or the conventional batch method. This makes the reactor design ideally suited for the systematic study of the mechanism of QD formation.

Experimental Section

The reactor was fabricated with standard silicon micromachining techniques. Channels were fashioned by deep reactive ion etching (DRIE) of a silicon wafer ($\varnothing = 15$ cm; thickness = 0.65 mm). An oxide layer (0.5 μm) was grown on the silicon surface, and the entire device was capped and sealed with an anodically bonded pyrex wafer (thickness = 0.76 mm). High-temperature fluidic connections were made by using glass solder (Diemat) to seal Kovar tubing to the reactor inlets. Standard 1/16-inch (1.6 mm) chromatography fittings (Upchurch) were used to connect the Kovar tubing to gas and liquid lines. Syringe pumps (Harvard PHD 2000 and KD Scientific 210) were used to deliver both precursor solutions and segmenting gas. A heated aluminum block in contact with the reaction section of the device was used for thermal control. The inlet and quenching regions were cooled with water-chilled aluminum blocks. Images of the reactor channel were taken with a consumer digital camera equipped with a macro lens and flash. For each flow condition, several hundred individual slug lengths were measured. The liquid fraction (liquid volume/total channel volume) was determined from the average slug lengths, and the mean residence time was calculated from the fraction and syringe pump flow rates.

The Cd and Se precursors were prepared as described previously with a few minor modifications.[12] All manipulations were performed under air-free conditions. Briefly, the Cd precursor was prepared by heating a suspension of cadmium 2,4-pentanedionate (1 mmol, 98 %, Alfa) in squalane (9 mL, 98 %, Alfa) and oleic acid (2.2 mmol, > 99 %, Alfa) at 150 °C for 10 min. The optically clear solution was then placed under vacuum at 100 °C for ≈ 1.5 h before the addition of 4 mL oleylamine (97 %, Pfaltz and Bauer). A stock solution of tri-*n*-octylphosphine selenide (TOPSe, 1.5 M) was prepared by dissolving an appropriate amount of selenium shot (99.999 %, Alfa) in tri-*n*-octylphosphine (TOP, 97 %, Strem). The Se precursor solution consisted of the suitable amount of TOPSe (1.5 M) diluted in squalane. The two precursor solutions were degassed thoroughly at 90 °C before loading into separate syringes.

Samples for the measurement of absorbance and PL spectra were prepared by diluting the raw QD solutions in hexanes. Optical absorption spectra were acquired with a Hewlett-Packard 8452 diode array spectrometer. Photoluminescence spectra were acquired with an Ocean Optics SD2000 fiber-optic spectrometer and a handheld UV lamp as an excitation source. Reaction yields were determined from the optical density at $\lambda = 350$ nm and the measured absorbance cross-section for CdSe QDs.[19]

Received: March 3, 2005

Keywords: microreactors · nanostructures · nanotechnology · quantum dots · segmented flow

---

[1] K. F. Jensen, *Chem. Eng. Sci.* **2001**, *56*, 293.
[2] K. Jähnisch, V. Hessel, H. Löwe, M. Baerns, *Angew. Chem.* **2004**, *116*, 410; *Angew. Chem. Int. Ed.* **2004**, *43*, 406.
[3] H. Song, J. D. Tice, R. F. Ismagilov, *Angew. Chem.* **2003**, *115*, 792; *Angew. Chem. Int. Ed.* **2003**, *42*, 768.
[4] A. Günther, S. A. Khan, M. Thalmann, F. Trachsel, K. F. Jensen, *Lab Chip* **2004**, *4*, 278.
[5] A. Günther, M. Jhunjhunwala, M. Thalmann, M. A. Schmidt, K. F. Jensen, *Langmuir* **2005**, *21*, 1547.
[6] I. Shestopalov, J. D. Tice, R. F. Ismagilov, *Lab Chip* **2004**, *4*, 316.
[7] C. B. Murray, D. J. Norris, M. G. Bawendi, *J. Am. Chem. Soc.* **1993**, *115*, 8706.
[8] L. Qu, Z. A. Peng, X. Peng, *Nano Lett.* **2001**, *1*, 333.
[9] Z. A. Peng, X. Peng, *J. Am. Chem. Soc.* **2001**, *123*, 183.
[10] M. G. Bawendi, N. E. Stott, US Patent Number 6,821,337, **2004**.
[11] For a review of microreactors for nanoparticle synthesis, see: J. deMello, A. deMello, *Lab Chip.* **2004**, *4*, 11N.
[12] B. K. H. Yen, N. E. Stott, K. F. Jensen, M. G. Bawendi, *Adv. Mater.* **2003**, *15*, 1858.
[13] H. Nakamura, Y. Yamaguchi, M. Miyazaki, H. Maeda, M. Uehara, P. Mulvaney, *Chem. Commun.* **2002**, 2844.
[14] The reported gas flow rates do not include the significant, although steady, gas leakage from the syringe and tubing fittings leading up to the reactor. We found this to be the case even with nominally gas-tight syringes. However, the slug lengths were measured directly from images taken of the reactor channel, so the reported mean residence times are accurate.
[15] The standard deviation of the *mean* of the liquid slug length gives rise to an uncertainty in the residence time: $\sigma_{t_r}/t_r = \sigma_l/(l_{avg}\sqrt{N})$ in which t_r is the residence time, l is the length of an individual slug, and N is the number of liquid slugs in the reactor (typically ≈ 300). As $\sigma_l/l_{avg} \approx 10\,\%$, $\sigma_{t_r}/t_r < 0.6\,\%$. In other words, the liquid slug length distribution does not contribute significantly to the overall residence time dispersion.
[16] From Ref. [5], we estimate the mixing time for segmented flow in our system to be $\approx 1\,\%$ of the average residence time. For the single-phase case, the diffusive mixing time can be $> 50\,\%$ of the average residence time depending on the flow rate.
[17] X. Peng, J. Wickham, A. P. Alivisatos, *J. Am. Chem. Soc.* **1998**, *120*, 5343.
[18] D. V. Talapin, A. L. Rogach, M. Haase, H. Weller, *J. Phys Chem. B* **2001**, *105*, 12278.
[19] C. A. Leatherdale, W.-K. Woo, F. V. Mikulec, M. G. Bawendi, *J. Phys. Chem. B* **2002**, *106*, 7619.